

Approximate residence time distribution of fully developed laminar flow in a straight rectangular channel

Martin Wörner

Karlsruhe Institute of Technology, Institut für Kern- und Energietechnik,
Postfach 3640, D-76021 Karlsruhe, Germany

E-Mail: martin.woerner@kit.edu

Abstract

For microfluidic applications the residence time distribution (RTD) of laminar flow in rectangular channels is of interest. The exact velocity profile for this type of flow consists of an infinite series and does not allow analytical evaluation of the RTD curve. In this paper we adopt a simpler binomial product profile which was proposed in literature and serves as good approximation. This allows us to determine in an analytical manner approximate expressions for the diffusion-free RTD of fully developed laminar flow in a straight rectangular channel of arbitrary aspect ratio. Since the evaluation of this RTD is computationally elaborate because it involves the Gauss hypergeometric function, we fit it by an empirical model which is suitable for engineering applications. We find that for a Newtonian fluid there is a narrowing of the RTD as the aspect ratio decreases from unity (square channel) to zero (parallel plates). We investigate the range of applicability of the diffusion-free RTD and show that it is a good estimation for liquids in a certain range of Reynolds numbers, whose limits depend on the length-to-hydraulic-diameter ratio of the channel.

Keywords: laminar flow, convective transport, dispersion, mixing, residence time distribution, rectangular channel

1. Introduction

Technical applications of chemical reaction engineering often rely on the interaction between chemical kinetics and fluid dynamics. In chemical reactors, the interplay between both processes is often characterized in terms of the reactors residence time distribution (RTD). The differential residence time distribution is a probability density function that describes the amount of time that fluid elements spend within the reactor. The RTD is of fundamental importance for estimating the yield and selectivity of any reaction in a certain reactor. Since Dankwerts (1953) analyzed in his seminal paper a number of important RTDs, this concept has become both a fundamental part of any textbook on chemical engineering and an important measure for characterization of any technical chemical reactor. A recent review on residence time theory and its applications in such diverse fields as chemical and biochemical process engineering, chromatography, medicine, geosciences and oceanography is given by Nauman (2008), while a comprehensive review with focus on straight and curved channels can be found in Nigam and Saxena (1986).

In classical large scale chemical reactors the fluid flow is usually turbulent and the RTD is often described by the tank-in-series model or the one-dimensional axial dispersion model (Levenspiel, 1999; Fogler, 1992). Within the last two decades the field of micro process engineering emerged, which utilizes miniaturized devices for process intensification. The lateral dimensions of reaction channels in such devices are typical on the order of 0.1 – 1 mm and the flow is predominantly laminar. The RTD caused by the velocity profile of fully developed laminar flow in a straight duct with no-slip boundary conditions is known only for certain cases, where the velocity profile depends on one coordinate only (i.e. the flow in a circular pipe and in a semi-infinite planar channel). In miniaturized devices, the size and geometry of the

channels is often determined by the fabrication techniques available for the microchannel manufacturing. Often the shape of the channel cross section is square or rectangular, but may be trapezoidal or triangular as well. The knowledge of the RTD of laminar flow in straight channels with non-circular cross-section is thus not only of academic interest but of significant practical importance. This holds not only for microreactors, but for microfluidic devices in general, where separation or mixing applications are frequent (e.g. in lab-on-a-chip systems). The relevance of the RTD in microfluidics devices is also reflected by a recently increasing number of experimental studies on this topic, see e.g. Trachsel et al. (2005), Lohse et al. (2008), Bošković and Loebbecke (2008), Stief et al. (2008), Adeosun and Lawal (2009), Cantu –Perez et al. (2009) to name a few. One of the problems limiting the effectiveness of microfluidics devices is the dispersion of material occurring in pressure-driven flow through microchannels. This makes it impossible to deliver sample material intact from one place in the microfluidics network to another without significant wastage (Vikhansky, 2009). It is evident that an analytical theory for the RTD imposed by the laminar velocity profile in non-circular channels would be very useful in order to further quantify the degree of mixing and dispersion in microfluidics processes.

In this paper we determine by an analytical procedure approximations to the pure convective (diffusion-free) RTD of fully developed laminar flow through a straight rectangular channel with arbitrary aspect ratio. To this end we approximate the exact laminar velocity profile in a rectangular channel, which involves an infinite series of trigonometric and hyperbolic functions, by a binomial product. This allows us to evaluate the RTD analytically and express it in terms of the Gauss hypergeometric function. We show that this RTD can well be approximated by a simpler model, which is suitable for engineering applications. We investigate the range of

applicability of the diffusion free RTD for practical applications and show that it may serve as good approximation for liquid systems in a certain range of Reynolds numbers.

The outline of the rest of this paper is as follows. In Section 2, we determine the RTD for the approximate velocity profile and present the simplified engineering model. In Section 3, we present results for the RTD of a Newtonian fluid in rectangular channels with different aspect ratio and investigate the range of applicability of the pure convective RTD theory. Finally, we conclude in Section 4.

2. Theory

2.1. Fundamental definitions of residence time distribution

For pure convective transport the cumulative residence time distribution function $F(t)$ describes the fraction of fluid that leaves the reactor with age less than t and is thus given by

$$F(t) = \frac{Q(t)}{Q_{\text{total}}} \quad (1)$$

Here, $Q(t)$ is the volumetric flow rate associated with a residence time t or lower and Q_{total} is the total volumetric flow rate. The differential residence time distribution function $E(t)$ is related to the cumulative residence time distribution by

$$E(t) = \frac{dF(t)}{dt} \quad (2)$$

Since $E(t)$ has unit of time^{-1} , the non-dimensional differential RTD

$$E_{\theta}(\theta) \equiv t_m E(t) \quad (3)$$

is more useful for comparing different reactors. E_{θ} is a function of the non-dimensional time $\theta \equiv t/t_m$ and fulfils the conditions

$$\int_0^{\infty} E_{\theta}(\theta) d\theta = \int_0^{\infty} \theta E_{\theta}(\theta) d\theta = 1 \quad (4)$$

Here,

$$t_m = \int_0^{\infty} t \cdot E(t) dt \quad (5)$$

is the mean or average residence time. For incompressible flow it is equal to the mean hydrodynamic residence time V / Q_{total} , where V is the reactor volume.

In this paper we consider the laminar flow of a Newtonian fluid with constant viscosity through a straight channel with constant cross section A and are interested in the RTD of a non-diffusive tracer substance. If the ratio of the length to the hydraulic diameter of the channel is sufficiently long then entrance effects can be ignored and the cumulative RTD can be computed via Eq. (1) from the fully developed velocity profile. For laminar flow through a pipe it is (Bosworth, 1948; Dankwerts, 1953)

$$E_{\theta_O}(\theta) = \begin{cases} 0 & \theta < \theta_{FO} \\ \frac{\theta_{FO}}{\theta^3} & \theta \geq \theta_{FO} \end{cases} \quad (6)$$

and

$$F_O(\theta) = \begin{cases} 0 & \theta < \theta_{FO} \\ 1 - \frac{\theta_{FO}}{2\theta^2} & \theta \geq \theta_{FO} \end{cases} \quad (7)$$

Here, θ_{FO} is the so-called first appearance time. This is the non-dimensional time when E_{θ} and F first differ from zero and is thus the dimensionless residence time of the fastest moving fluid. θ_F is equal to the ratio between the mean and maximum velocity U_m / U_{max} , which takes a value of $\theta_{FO} = 0.5$ for a circular pipe. For the laminar flow between parallel plates (and in a falling film) it is (Levenspiel, 1979)

$$E_{\theta_{\parallel}}(\theta) = \begin{cases} 0 & \theta < \theta_{\text{F}\parallel} \\ \frac{1}{2} \frac{\theta_{\text{F}\parallel}}{\theta^3} \left(1 - \frac{\theta_{\text{F}\parallel}}{\theta}\right)^{-\frac{1}{2}} & \theta \geq \theta_{\text{F}\parallel} \end{cases} \quad (8)$$

and

$$F_{\parallel}(\theta) = \begin{cases} 0 & \theta < \theta_{\text{F}\parallel} \\ \frac{2}{3\theta_{\text{F}\parallel}} \left(1 + \frac{\theta_{\text{F}\parallel}}{2\theta}\right) \left(1 - \frac{\theta_{\text{F}\parallel}}{\theta}\right)^{\frac{1}{2}} & \theta \geq \theta_{\text{F}\parallel} \end{cases} \quad (9)$$

where $\theta_{\text{F}\parallel} = 2/3$. Since E_{θ} and F_{θ} are always zero for $\theta < \theta_{\text{F}}$, we give in the sequel the functional relationships for $\theta \geq \theta_{\text{F}}$ only and denote both by E_{θ}^+ and F^+ , respectively.

2.2. RTD in a rectangular channel with Purday's velocity profile

We consider a rectangular channel with half-width w and half-height h as displayed in Fig. 1, where we assume $w \geq h > 0$. The origin of the coordinate system is located in the channel center so that $-w \leq z \leq w$ and $-h \leq y \leq h$. Then, the laminar Poiseuille velocity profile of a Newtonian fluid with constant viscosity is (Holmes and Vermeulen, 1968; Shah and London, 1978)

$$u(y, z) = U_{\max} \frac{\sum_{k=1,3,5}^{\infty} \frac{(-1)^{(k-1)/2}}{k^3} \left[1 - \frac{\cosh(k\pi y / 2w)}{\cosh(k\pi h / 2w)}\right] \cos(k\pi z / 2w)}{\sum_{k=1,3,5}^{\infty} \frac{(-1)^{(k-1)/2}}{k^3} \left[1 - \frac{1}{\cosh(n\pi h / 2w)}\right]} \quad (10)$$

Since this velocity profile is given by an infinite series, an analytical evaluation of the residence time distribution via Eq. (1) seems impossible. Saxena and Nigam (1983) have numerically computed the RTD for a square channel using the velocity profile given by Eq. (10) with $h = w$. The numerically computed RTD functions were fitted to Nauman's (1977) model for diffusion-free RTD as

$$F_{\square}^+(\theta) = 1 - \frac{0.2316}{\theta^{1.908}} - \frac{0.0111}{\theta^2} \quad (11)$$

for $\theta \geq \theta_{\text{F0}} = 0.477$.

(appropriate place for Figure 1)

Since Eq. (10) involves considerable computational complexity, Purday (1949) proposed the following approximation

$$u(Y, Z) = U_{\text{max}} (1 - Y^n)(1 - Z^m) = \frac{m+1}{m} \frac{n+1}{n} U_{\text{m}} (1 - Y^n)(1 - Z^m) \quad (12)$$

Here, it is $Y \equiv y/h$, $Z \equiv z/w$. The values of the exponents n and m depend on the channel aspect ratio $\chi \equiv h/w$, where $0 < \chi \leq 1$. At this stage we let these relationships undefined and refer to Section 3. In the present subsection we derive, to our knowledge for the first time, the RTD for the velocity profile given by Eq. (12).

For this purpose we consider the curves $Z_\lambda = Z(Y, \lambda)$ where $u = u_\lambda = \lambda U_{\text{max}}$ is constant. Here, λ is in the range $0 < \lambda \leq 1$. From Eq. (12) we obtain

$$Z_\lambda = \left(1 - \frac{\lambda}{1 - Y^n}\right)^{\frac{1}{m}} = \left(\frac{Y_{\text{max},\lambda}^n - Y^n}{1 - Y^n}\right)^{\frac{1}{m}} \quad (13)$$

where $Y_{\text{max},\lambda} \equiv (1 - \lambda)^{1/n}$ is the value of Y for $Z = 0$.

We consider an axial portion of the rectangular channel with length L . Then, the minimum and mean residence time are $t_{\text{F}} = L/U_{\text{max}}$ and $t_{\text{m}} = L/U_{\text{m}}$, respectively.

The residence time of fluid elements moving with velocity u_λ is

$$t = L/\lambda U_{\text{max}} = t_{\text{min}}/\lambda \text{ so that the non-dimensional residence time can be expressed}$$

as

$$\theta \equiv \frac{t}{t_{\text{m}}} = \frac{1}{\lambda} \frac{U_{\text{m}}}{U_{\text{max}}} = \frac{\theta_{\text{F0}}}{\lambda} \quad (14)$$

For the Purday velocity profile of Eq. (12) we have

$$\theta_{\text{F0}} = \frac{t_{\text{F}}}{t_{\text{m}}} = \frac{U_{\text{m}}}{U_{\text{max}}} = \frac{m}{m+1} \frac{n}{n+1} \quad (15)$$

The flow rate $Q(t)$ associated with fluid moving with a velocity $u \geq \lambda U_{\max}$ is

given by

$$Q(t) = \iint_{A_\lambda} u dA = 4wh \int_0^{Y_{\max,\lambda}} \int_0^{Z_\lambda} U_{\max} (1-Y^n)(1-Z^m) dZ dY \quad (16)$$

We perform the integration with respect to Z and obtain with $Q_{\text{total}} = 4whU_m$ from

Eq. (1) the result

$$F_{\square}^+ = \frac{1}{\theta_{F_{\square}}} \int_0^{Y_{\max,\lambda}} (1-Y^n) Z_\lambda \left(1 - \frac{Z_\lambda^m}{m+1} \right) dY \quad (17)$$

Inserting Eq. (13) in Eq. (17) gives

$$F_{\square}^+ = \frac{1}{\theta_{F_{\square}}} \frac{1}{m+1} \int_0^{Y_{\max,\lambda}} \left(\frac{Y_{\max,\lambda}^n - Y^n}{1-Y^n} \right)^{\frac{1}{m}} (m+1 - mY^n - Y_{\max,\lambda}^n) dY \quad (18)$$

and with the substitution $s \equiv (Y / Y_{\max,\lambda})^n$

$$F_{\square}^+ = \frac{1}{\theta_{F_{\square}}} \frac{1}{n} \frac{m+1 - Y_{\max,\lambda}^n}{m+1} Y_{\max,\lambda}^{\frac{m+n}{m}} \int_0^1 s^{\frac{1}{n}-1} (1-s)^{\frac{1}{m}} (1 - Y_{\max,\lambda}^n s)^{-\frac{1}{m}} \left(1 - \frac{mY_{\max,\lambda}^n}{m+1 - Y_{\max,\lambda}^n} s \right) ds \quad (19)$$

With $\lambda = \theta_{F_{\square}} / \theta$ it is $Y_{\max,\lambda} = (1 - \theta_{F_{\square}} / \theta)^{1/n}$ and Eq. (19) becomes

$$F_{\square}^+ = \frac{1}{\theta_{F_{\square}}} \frac{1}{n} \frac{m}{m+1} \left(1 - \frac{\theta_{F_{\square}}}{\theta} \right)^{\frac{m+n}{mn}} \left[\left(1 + \frac{1}{m} \frac{\theta_{F_{\square}}}{\theta} \right) J_1 - \left(1 - \frac{\theta_{F_{\square}}}{\theta} \right) J_2 \right] \quad (20)$$

where

$$J_1 \equiv \int_0^1 s^{\frac{1}{n}-1} (1-s)^{\frac{1}{m}} \left[1 - \left(1 - \frac{\theta_{F_{\square}}}{\theta} \right) s \right]^{\frac{1}{m}} ds \quad (21)$$

$$J_2 \equiv \int_0^1 s^{\frac{1}{n}} (1-s)^{\frac{1}{m}} \left[1 - \left(1 - \frac{\theta_{F_{\square}}}{\theta} \right) s \right]^{-\frac{1}{m}} ds$$

The integrals J_1 and J_2 can be evaluated by the following integral representation

(Andrews et al., 1999, p. 65)

$$\int_0^1 s^{\beta-1} (1-s)^{\gamma-\beta-1} (1-sx)^{-\alpha} ds = \frac{\Gamma(\beta)\Gamma(\gamma-\beta)}{\Gamma(\gamma)} {}_2F_1(\alpha, \beta; \gamma; x) \quad (22)$$

Here, Γ is the Gamma function and

$$\begin{aligned}
{}_2F_1(\alpha, \beta; \gamma; x) &= \frac{\Gamma(\gamma)}{\Gamma(\alpha)\Gamma(\beta)} \sum_{k=0}^{\infty} \frac{\Gamma(\alpha+k)\Gamma(\beta+k)}{\Gamma(\gamma+k)} \frac{x^k}{k!} \\
&= 1 + \frac{\alpha\beta}{\gamma} \frac{x}{1!} + \frac{\alpha(\alpha+1)\beta(\beta+1)}{2!\gamma(\gamma+1)} \frac{x^2}{2!} + \dots
\end{aligned} \tag{23}$$

is the Gauss hypergeometric function. In this paper we assume that α , β and $\gamma > \alpha + \beta$ are real parameters with none of them being zero or a negative integer.

Then, the series (23) converges for $|x| < 1$ (Andrews, 1998, p. 361). In the Appendix we list some properties of the Gauss hypergeometric function that will be used in the sequel.

For shortage of notation we define $a \equiv 1/m$, $b \equiv 1/n$, $c \equiv 1+a+b$ and

$\Theta \equiv 1 - \theta_{\text{Fo}} / \theta$ so that Eq. (20) becomes

$$F_{\square}^+ = \frac{1}{\theta_{\text{Fo}}} \frac{b}{1+a} \Theta^{a+b} \left[(1+a(1-\Theta))J_1 - \Theta J_2 \right] \tag{24}$$

By comparing J_1 and J_2 with Eq. (22) we obtain

$$J_1 = \frac{\Gamma(1+a)\Gamma(b)}{\Gamma(c)} {}_2F_1(a, b; c; \Theta) \tag{25}$$

and

$$\begin{aligned}
J_2 &= \frac{\Gamma(1+a)\Gamma(1+b)}{\Gamma(1+c)} {}_2F_1(a, b+1; c+1; \Theta) \\
&= \frac{\Gamma(1+a)\Gamma(b)}{\Gamma(c)} \left[{}_2F_1(a, b, c; \Theta) - \frac{c-b}{c} {}_2F_1(a, b; c+1; \Theta) \right]
\end{aligned} \tag{26}$$

In Eq. (26) we used the property of the Gamma function $\Gamma(x+1) = x\Gamma(x)$ and relation (A.6).

Introducing Eq. (25) and Eq. (26) in Eq. (24) and rearranging yields

$$\begin{aligned}
F_{\square}^+ &= \frac{1}{\theta_{\text{Fo}}} \frac{\Gamma(1+a)\Gamma(1+b)}{\Gamma(c)} \Theta^{a+b} \left[(1-\Theta) {}_2F_1(a, b; c; \Theta) + \frac{\Theta}{c} {}_2F_1(a, b; c+1; \Theta) \right] \\
&= \frac{ab}{\theta_{\text{Fo}}} \sum_{k=0}^{\infty} \frac{\Gamma(a+k)\Gamma(b+k)}{\Gamma(c+k)} \left(1 - \frac{c+k-1}{c+k} \Theta \right) \frac{\Theta^{a+b+k}}{k!}
\end{aligned} \tag{27}$$

respectively

$$F_{\square}^+ = \frac{1}{\theta_{F_{\square}}} \frac{1}{m} \frac{1}{n} \sum_{k=0}^{\infty} \frac{1}{k!} \frac{\Gamma(m^{-1}+k)\Gamma(n^{-1}+k)}{\Gamma(1+m^{-1}+n^{-1}+k)} \left[1 - \frac{m^{-1}+n^{-1}+k}{m^{-1}+n^{-1}+k+1} \left(1 - \frac{\theta_{F_{\square}}}{\theta} \right) \right] \left(1 - \frac{\theta_{F_{\square}}}{\theta} \right)^{m^{-1}+n^{-1}+k} \quad (28)$$

The differential RTD can be computed via

$$E_{\theta_{\square}}^+ = \frac{dF_{\square}^+(\theta)}{d\theta} = \frac{dF_{\square}^+(\Theta)}{d\Theta} \frac{d\Theta}{d\theta} = \frac{(1-\Theta)^2}{\theta_{F_{\square}}} \frac{dF_{\square}^+(\Theta)}{d\Theta} \quad (29)$$

The result reads

$$\begin{aligned} E_{\theta_{\square}}^+ &= \frac{1}{\theta_{F_{\square}}} \frac{\Gamma(2+a)\Gamma(2+b)}{\Gamma(1+a+b)} (1-\Theta)^3 \Theta^{a+b-1} \left[b {}_2F_1(a, b; c; \Theta) + a {}_2F_1(a+1, b; c; \Theta) \right] \\ &= \frac{ab}{\theta_{F_{\square}}^2} (1-\Theta)^3 \sum_{k=0}^{\infty} \frac{\Gamma(a+k)\Gamma(b+k)}{\Gamma(a+b+k)} \frac{\Theta^{a+b+k-1}}{k!} \end{aligned} \quad (30)$$

and in terms of θ

$$E_{\theta_{\square}}^+ = m^{-1}n^{-1} \frac{\theta_{F_{\square}}}{\theta^3} \sum_{k=0}^{\infty} \frac{1}{k!} \frac{\Gamma(m^{-1}+k)\Gamma(n^{-1}+k)}{\Gamma(m^{-1}+n^{-1}+k)} \left(1 - \frac{\theta_{F_{\square}}}{\theta} \right)^{m^{-1}+n^{-1}+k-1} \quad (31)$$

It can be shown that $E_{\theta_{\square}}^+(\theta)$ fulfils both conditions of Eq. (4). The non-dimensional

variance of this RTD is given by

$$\sigma_{\theta_{\square}}^2 \equiv \int_0^{\infty} (\theta-1)^2 E_{\theta_{\square}}^+ d\theta = \int_{\theta_{F_{\square}}}^{\infty} (\theta-1)^2 E_{\theta_{\square}}^+ d\theta \quad (32)$$

Evaluation of this integral yields $\sigma_{\theta_{\square}}^2 = \infty$, as is typical for non-diffusive laminar

flows (Nauman, 1977).

2.3. Simplified engineering RTD model

The Gauss hypergeometric function must be evaluated numerically. For engineering applications it is therefore useful to approximate the differential and cumulative RTD by simpler expressions. A semi-empirical model based on characteristic parameters of the RTD (mean, minimum, maximum residence time) and on an empirical exponent to permit better fitting was proposed by Ham and Platzer (2004). However, the model turned out not to be useful in the present context because it involves the maximum residence time which tends to infinity here. So a

new simplified model is proposed in this subsection.

The differential RTD for a planar channel in Eq. (8) and Eq. (31) suggests a fit by a family of curves of the form

$$\tilde{E}_\theta^+ = \frac{A}{\theta^p} \left(1 - \frac{\theta_F}{\theta}\right)^{-q} \quad (33)$$

While this model has four parameters, due to the two conditions from Eq. (4) only two parameters can be chosen freely. We select θ_F , because it has as has non-dimensional first appearance time a clear physical meaning, and p , where we require $p > 2$. The conditions of Eq. (4) yield

$$\begin{aligned} \int_0^\infty \tilde{E}_\theta^+ d\theta &= \frac{A}{p-1} \theta_F^{1-p} {}_2F_1(p-1, q, p; 1) = 1 \\ \int_0^\infty \theta \tilde{E}_\theta^+ d\theta &= \frac{A}{p-2} \theta_F^{2-p} {}_2F_1(p-2, q, p-1; 1) = 1 \end{aligned} \quad (34)$$

With Eq. (A.2) it follows

$$\tilde{E}_\theta^+ = \frac{\Gamma(1+(p-2)\theta_F^{-1})}{\Gamma(p-1)\Gamma((p-2)(\theta_F^{-1}-1))} \frac{\theta_F^{p-1}}{\theta^p} \left(1 - \frac{\theta_F}{\theta}\right)^{(p-2)(\theta_F^{-1}-1)-1} \quad (35)$$

The corresponding cumulative RTD is given by

$$\tilde{F}^+ = 1 - \frac{\Gamma(1+(p-2)\theta_F^{-1})}{\Gamma(p)\Gamma((p-2)(\theta_F^{-1}-1))} \left(\frac{\theta_F}{\theta}\right)^{p-1} {}_2F_1(p-1, 1-(p-2)(\theta_F^{-1}-1), p; \frac{\theta_F}{\theta}) \quad (36)$$

Since θ_F is already determined by Eq. (15), only p remains as free parameter. We

note that for $p < 1 + (1 - \theta_F)^{-1}$ it is $q > 0$ and the value of $\tilde{E}_\theta^+(\theta = \theta_F)$ is infinite,

while it is finite for larger values of p . Eq. (8) and Eq. (31) suggest $p = 3$. Then Eq.

(35) becomes

$$\tilde{E}_\theta^+ = \frac{1 - \theta_F}{\theta^3} \left(1 - \frac{\theta_F}{\theta}\right)^{\theta_F^{-1}-2} \quad (37)$$

For $\theta_F = \theta_{F0} = 0.5$ Eq. (37) becomes identical to the RTD for laminar flow in a pipe (cf. Eq. (6)), while for $\theta_F = \theta_{F1} = 2/3$ it becomes identical to the RTD for laminar flow between parallel plates (cf. Eq. (8)).

3. Results and discussion

3.1. Laminar flow of a Newtonian fluid in a rectangular channel

To utilize the results of the previous section, we require relations for the dependence of the exponents m and n in Eq. (12) on the aspect ratio χ . Purday (1949) used $n = 2$ and applied the principle of minimum energy dissipation to obtain m for five distinct values of χ , see Table 1. Natarajan and Lakshmanan (1972) solved the momentum equation by a finite difference method for eight different values of the aspect ratio in the range $0.05 \leq \chi \leq 1$ and matched the velocity profile to the empirical Eq. (12). They proposed the relations

$$n = \begin{cases} 2 & \text{for } 0 \leq \chi \leq 1/3 \\ 2 + 0.3(\chi - 1/3) & \text{for } 1/3 \leq \chi \leq 1 \end{cases} \quad (38)$$

$$m = 1.7 + 0.5\chi^{-1.4}$$

and report good agreement of the respective velocity profiles with the experimental data of Holmes and Vermeulen (1968) for different values of the aspect ratio. Table 1 lists the values of m and n which arise from Eq. (38) for certain values of χ .

Once m and n are given, the first appearance time θ_{F0} can be computed by Eq. (15). The results for θ_{F0} are listed in Table 1 and are compared with the exact values from the velocity profile of Eq. (10) (see, Shah and London, 1978). Fig. 2 displays θ_{F0} versus χ in graphical form and compares the values of Purday (1949) and Natarajan and Lakshmanan (1972) with the correlation

$$\frac{U_{\max}}{U_m} = \frac{1}{\theta_{F\Box}} = \frac{3}{2} \left(1 + 0.546688\chi + 1.552013\chi^2 - 4.059427\chi^3 + 3.214927\chi^4 - 0.857313\chi^5 \right) \quad (39)$$

proposed by Spiga and Morini (1994). These authors determined exact values of U_{\max}/U_m for ten different aspect ratios in the range $0 \leq \chi \leq 1$ and fitted these data by Eq. (39) with an accuracy of 0.06%. Fig. 2 indicates that the values for m and n proposed by Purday (1949) result in good agreement of $\theta_{F\Box}$ with the exact values only for $\chi \leq 1/3$. Instead, Eq. (38) yields reasonable accurate results for all aspect ratios as the approximate values of $U_{\max}/U_m = \theta_F^{-1}$ are within 0.9% of the exact results in Table 1. However, with today's computer power a careful repetition of the study of Natarjan and Lakshmanan (1972) may yield even better fits for m and n and thus $\theta_{F\Box}$. Here, we use Eq. (30) and Eq. (27) in conjunction with Eq. (38) to determine the RTD for different values of the aspect ratio. We denote this RTD as the Purday-Natarjan-Lakshmanan (PNL) RTD. For computation of the PNL-RTD the Gauss hypergeometric function needs to be evaluated. For this purpose we use the FORTRAN program hyp.f of Forrey (1997).

(appropriate place for Figure 2)

In Fig. 3 we show the results for the cumulative and differential PNL-RTD for rectangular channels with different aspect ratio and compare these curves with the RTD for laminar flow in a circular channel and between parallel plates. Interestingly, for $\theta = \theta_F$ the value of E_θ is finite for a circular channel but is infinite for the planar and rectangular channel, regardless of the aspect ratio. Characteristic for the RTD of the rectangular channels is the sharp drop from the infinite value of $E_\theta(\theta)$ at $\theta = \theta_F$ towards values of less than 1 for $\theta = \theta_F + 0.3$. As the aspect ratio decreases from unity toward zero, the RTD shifts to the right due to the increase of θ_F from 0.477

toward 0.667, see Table 1. Fig. 3 shows that for a rectangular channel the RTD is the widest for a square channel and the narrowest for a planar channel. Notably, the difference of the RTDs for a square channel and a rectangular channel with $\chi = 0.5$ is smaller than that for a rectangular channel with $\chi = 0.125$ and the flow between parallel plates. It is also interesting to note that for $\theta > \theta_F$ the RTD for a rectangular channel with aspect ratio $\chi = 0.5$ is very similar to that for a circular channel.

Natarajan and Lakshmanan (1972) note that the exponent m in Eq. (38) becomes very large for low values of χ so that it is $1 - Z^m \approx 1$ except for points near the wall. Then Eq. (12) becomes $u/U_{\max} = 1 - Y^n$, which is the same as for flow between parallel plates. Though not shown in Fig. 3, we evaluated F_{\square}^+ as given by Eq. (27) for values of χ smaller than 0.125. We found that in the absence of diffusion the RTD for a rectangular channel becomes virtually identical to that for the flow between parallel plates if $\chi \leq 0.02$. This result is interesting, since it is known that in the presence of molecular diffusion the Taylor dispersion of a flow between two infinite plates and in an infinite thin rectangular channel differs by a factor of about eight (Doshi et al., 1978; Desmet and Baron, 2002). Thus in the presence of diffusion, the very small side walls of the rectangular channel have an enormous influence on the dispersion.

Characteristic for diffusion-free laminar flows is the long tail of the RTD which makes all moments of degree two and higher infinite (Nauman, 1977). While in the main diagram of Fig. 3 b) the different RTD profiles collapse to a single curve for $\theta > 1.5$, the log-log inset graphics shows that the profiles are slightly different for large values of θ . However, the slope in the rectangular channel is similar to that for a circular pipe and parallel plates, which obey a relationship $E_{\theta} \propto \theta^{-3}$ for large

values of θ .

(appropriate place for Figure 3)

Fig. 3 shows that the RTD gets broader as the aspect ratio increases from zero to one, because θ_F decreases as χ increases (cf. Fig. 2). Saxena and Nigam (1983) explained the broader RTD in a square channel as compared to a circular channel by the fact that - for the same cross-sectional area - the wetted periphery in case of a square channel is $2/\sqrt{\pi} = 1.128$ times higher. This will cause a higher fraction of the fluid to be at lower axial velocity. Therefore for the same cross-sectional area and volumetric flow rate, the fluid elements flowing at the centre of the tube will move at a faster rate to compensate the higher fraction of fluid at lower velocity. If we compare a rectangular channel with a square channel of the same cross-sectional area, then the ratio between the wetted perimeter of both channels is

$P_{\square} / P_{\square} = 0.5(1 + \chi) / \sqrt{\chi}$. This ratio is larger than one for $\chi < 1$ and tends to infinity for $\chi \rightarrow 0$. Thus, for a given cross-sectional area the periphery of a rectangular channel is always larger than that of square channel. Nevertheless, the RTD of the square channel is broader than that of the rectangular channel. This renders the argumentation of Saxena and Nigam (1983) invalid. By Eq. (14) it is $\theta_F = U_m / U_{\max}$ so that the broadness of the non-dimensional RTD is only determined by the ratio between the mean and maximum velocity in the channel.

We now investigate in how far the exact PNL-RTD can be fitted by the model of Eq. (35). For this purpose we first consider a square channel and compare in Fig. 4 the exact PNL-RTD with the model of Saxena and Nigam (1983) given by the derivative of Eq. (11) and with the present model for different values of p , namely $p = 3$, $p = 2.8$ and $p = 2.5$. For a square channel it is $m = n = 11/5$ and

$\theta_{F_{\square}} = 121/256$ so that for $p = 3$ it is $q = -14/121$. Therefore the exponent $-q$ in model (35) is positive and the RTD is finite for $\theta = \theta_{F_{\square}}$ whereas the RTD based on the Gauss hypergeometric function is infinite, see Fig. 4. For this reason the present model with $p = 3$ is not a good fit for a square channel. The condition that the RTD is infinite for $\theta = \theta_F$ is $p < (2 - \theta_F) / (1 - \theta_F)$, i.e. for a square channel $p < 2.896$. For $p = 2.5$ we obtain $q = 0.44215$, which is very close to 0.5 (i.e. the exponent for the parallel plates case). However, the performance of the model for this value of p is poor, see Fig. 4. The model of Saxena and Nigam performs much better, but has the disadvantage that it yields a finite value for $\theta = \theta_F$ which is not correct. For $p = 2.8$ Eq. (35) becomes

$$\tilde{E}_{\theta}^{+}(\theta) = \frac{0.39814}{\theta^{2.8}} \left(1 - \frac{0.47266}{\theta} \right)^{-0.10744} \quad (40)$$

Fig. 4 shows that an excellent agreement with the PNL-RTD is obtained by Eq. (40), so that this equation is proposed as a simplified model for the diffusion-free RTD in a square channel.

(appropriate place for Figure 4)

We determined suitable value of p for seven different values of the aspect ratio in the range $0 < \chi \leq 1$ and found that an excellent agreement between the PNL-RTD and the simplified model is obtained for all cases when p is computed as

$$p(\chi) = 3 - 0.4\chi + 0.2\chi^2 \quad (41)$$

Thus, the differential RTD for the diffusion-free laminar flow of a Newtonian fluid in a rectangular channel of arbitrary aspect ratio is well described by Eq. (35) when m and n are computed by Eq. (38), $\theta_{F_{\square}}$ by Eq. (15) and p by Eq. (41).

In recent years several papers were published where the diffusion-free RTD for

laminar flow in small square or rectangular channels is determined by Eulerian CFD simulations and Lagrangian tracking of mass-less particles, both for single phase flow (e.g. Aubin et al., 2009) and for two-phase flow (e.g. Wörner et al., 2007). Aubin et al. (2009) determined the RTD for Newtonian and shear-thinning fluids for seven different values of aspect ratios in the range $0.05 \leq \chi \leq 1$. In their particle tracking method they applied a restitution coefficient of unity to the microchannel walls in order to avoid particle trajectories being trapped near the walls, where the local velocity is close to zero. They note that less than 2% of the particles are stopped between the channel inlet and outlet. For all differential RTD curves obtained, the maximum value and the variance σ_θ^2 are finite. Aubin et al. (2009) utilize these values of σ_θ^2 to determine a reactor Peclet number in order to quantify the degree of axial dispersion by the laminar flow. From their results they conclude that in order to narrow the RTD and to reduce the axial dispersion, microchannels with aspect ratio $\chi \leq 0.3$ should be used. While this conclusion is in full accordance with the results of the present theoretical study, it is evident that the finite value of σ_θ^2 is an artifact. It is only due to the neglect of the 2% of particles in near wall regions with very high residence time that the value of σ_θ^2 is finite and not infinite as it should be for a diffusion-free laminar flow. As a consequence, the values reported by Aubin et al. (2009) for the reactor Peclet numbers and the axial dispersion coefficients in rectangular channels with different aspect ratio are not physical but are only due to deficiencies of particle tracking methods for determining the RTD of diffusion-free processes. In the conclusions of his review, Nauman (2008) notes that modern CDF codes are actually quite sloppy with respect to calculate the RTD and speculates that codes have difficulties with the low velocities near solid boundaries.

It is evident that for comparison with experimental RTD data obtained by tracer

experiments, CFD methods which incorporate diffusion in some way may yield more reliable RTD curves than pure convective models. Cantu –Perez et al. (2009) present a particle-tracking method which accounts for diffusion by a stochastic random walk process, and compare the RTD in rectangular microchannels with and without herringbone structures. A recent example for the more traditional way to account for the influence of diffusion on the RTD by solving the unsteady chemical species transport equation can be found in Adeosun and Lawal (2009), where the RTD in a microchannel T-junction is studied numerically and experimentally.

3.2. Range of validity of convective RTD model

The results obtained in the previous section may find practical application, provided that the assumptions of fully developed flow and negligible influence of molecular diffusion are fulfilled. The laminar flow can be considered as fully developed if the channel length L is significantly larger than the entrance length L_e . Morini (2004) used the approach of McComas (1967) and determined the entrance length for laminar flow in a rectangular channel from his numerical results for the fully developed velocity profile. We found that the data of Morini (2004) for 13 different values of the aspect ratio in the range $0 \leq \chi \leq 1$ can well be fitted the relation

$$\frac{L_e}{d_h Re_h} = 0.033 - 0.0314 \left[1 + \exp\left(\frac{\chi - 0.305}{0.165}\right) \right]^{-1} \quad (42)$$

Here, d_h is the hydraulic diameter and $Re_h \equiv d_h U_m / \nu$ is the Reynolds number.

Though experimentally determined values of the entrance length are usually larger than suggested by the theory of McComas (1967), Eq. (42) nevertheless indicates that the entrance length is much smaller in low aspect ratio rectangular channels than in a square channel.

We now consider the second assumption, namely that of negligible molecular diffusivity D of the chemical species. A detailed investigation on the influence of diffusion on the RTD of laminar flow in a circular pipe is given by Bosworth (1948). He notes that axial and radial diffusion modifies the differential RTD in certain ways. Due to longitudinal (axial) diffusion, some molecules have a residence time less than θ_F (the first appearance time in the absence of diffusion). Furthermore, the sharp cut-off at the lower end of the differential RTD curve is replaced by one which is more gradual. In addition, as shown by Nauman (1977), the presence of diffusion causes an exponential tail of the RTD and reduces all moments to finite values. Bosworth (1948) showed that for laminar flow through a straight tube of diameter d the effect of longitudinal diffusion is negligible for $L > 360\sqrt{t_F D}$ and that of radial diffusion for $d > 36\sqrt{t_F D}$. The condition for longitudinal diffusion may be readily applied to a rectangular channel and yields

$$\frac{L}{d_h} > \frac{129600\theta_F}{Pe_h} \quad (43)$$

where $Pe_h \equiv d_h U_m / D$ is the Peclet number. Transversal diffusion in a rectangular channel occurs in y and z direction. The more stringent condition for the neglect of transversal diffusion arises from the shorter channel dimension. Thus, we replace in Bosworth's criterion d by $2h = d_h(1 + \chi) / 2$ and obtain

$$\frac{L}{d_h} < \frac{(1 + \chi)^2}{5184\theta_F} Pe_h \quad (44)$$

If we require $L > 10L_e$ then the conditions (42), (43) and (44) can be combined as

$$\max \left\{ 0.33 - 0.314 \left[1 + \exp \left(\frac{\chi - 0.305}{0.165} \right) \right]^{-1}, \left(\frac{360}{Re_h} \right)^2 \frac{\theta_F}{Sc} \right\} < \frac{1}{Re_h} \frac{L}{d_h} < \frac{(1 + \chi)^2}{5184} \frac{Sc}{\theta_F} \quad (45)$$

Thus, the range of applicability of the present approximate RTD theory depends to a large extent on the value of the Schmidt number $Sc \equiv \nu / D$. For gases and gas mixtures the Schmidt number ranges from about 0.2 to 3 (Bird et al., 2002) and the conditions in (45) are never fulfilled for laminar flow since the effect of diffusion is always significant. For low viscosity liquids like water it is $Sc \approx 1000$ and the conditions of inequality (45) are met over a certain range of Reynolds numbers, see below. For liquid mixtures values of Sc up to 37000 are observed (Shaw and Hanratty, 1977) while for high viscosity liquids values as high as $Sc = 1.4 \times 10^6$ are reported (Trivedi and Vasudeva, 1974). Then, the range of validity of the pure convective RTD theory is further extended.

From Eq. (45) we have three conditions that must be simultaneously fulfilled so that the diffusion-free RTD theory may be applied. A fourth condition arises from the demand that the flow is laminar. The question of laminar/turbulent transition of liquid flows in microchannels has motivated a large number of experimental studies which are discussed controversially in literature, see Hetsroni et al. (2005) for a review. Recent experiments performed by Wibel and Ehrhard (2009) in smooth rectangular microchannels with three different aspect ratios (1, 0.5, 0.2) show that –similar to macroscopic channels – the laminar/turbulence transition occurs in the Reynolds number range 1900–2200. However, for aspect ratios departing from unity, the onset of turbulence occurs at larger values of Re_h , and the width of the transition range increases. This implies that there exists no unique transition range for the three microchannels of different aspect ratio (Wibel and Ehrhard, 2009). In the sequel we assume therefore that the flow is laminar for $Re_h < 1900$.

In a log-log representation with L/d_h as abscissa and Re_h as ordinate, the three conditions in (45) and that of laminar flow represent four lines, which enclose an

area where the present convective RTD model may be used. In Fig. 5 we display this area for a square channel and for parallel plates for $Sc = 1000$. It appears that the assumption of negligible transversal diffusion defines an upper limit for L/d_h , while negligible longitudinal diffusion is the relevant lower limit for L/d_h at small values of Re_h and fully developed flow at large values of Re_h . It appears that with decrease of χ the range of applicability of the convective RTD model shifts to larger values of Re_h and lower values for L/d_h . However, the range of applicability of the pure convective RTD model is rather limited when the criteria of Bosworth (1948) are applied.

A simple comparison of the diffusive and convective time scales indicates that the effects of longitudinal and transversal diffusion are negligible for $L/d_h \gg 1/Pe_h$ and $L/d_h \ll (1+\chi)^2 Pe_h/4$, respectively. Probstein (2003) uses a ratio 10:1 to define “large/small compared with”. The conditions (43) and (44) from Bosworth’s analysis are, however, much more stringent and suggest a ratio of up to 86400:1 and 864:1 for longitudinal and transversal diffusion, respectively. If we adopt for the longitudinal direction a ratio of 1:10000 and for the transversal direction a ratio of 250:1 then the conditions (45) become

$$\max \left\{ 0.33 - 0.314 \left[1 + \exp \left(\frac{\chi - 0.305}{0.165} \right) \right]^{-1}, \frac{1000}{Re_h^2 Sc} \right\} < \frac{1}{Re_h} \frac{L}{d_h} < \frac{(1+\chi)^2}{1000} Sc \quad (46)$$

These conditions are much less restrictive than those in Eq. (45) so that the range of applicability of the diffusion-free RTD theory is enlarged, see Fig. 5. We expect that conditions (46) are sufficiently accurate for engineering applications, so that they can be used to estimate for given values of Sc and L/d_h the range of Reynolds numbers where the diffusion-free theory may be applied.

(appropriate place for Figure 5)

4. Conclusions

From the present theoretical investigation the following conclusions can be drawn:

1. Eq. (28) and Eq. (31) in combination with Eq. (38) and Eq. (15) represent a reasonable accurate approximation to the cumulative and differential diffusion-free RTD for fully developed laminar flow of a Newtonian fluid in a straight rectangular channel with arbitrary aspect ratio. Alternatively, the simplified model given by Eq. (35) can be used in combination with Eqs. (38), (15) and (41).
2. For the fully developed flow of a Newtonian fluid in a rectangular channel there is a narrowing of the RTD as the aspect ratio decreases from unity (square channel) to zero (parallel plates). For mixing applications, a narrow RTD is preferred so low aspect ratio channels are recommended.
3. The criteria of Eq. (46) define conditions where the present RTD theory for diffusion-free fully developed laminar flow in a rectangular channel is valid. These criteria can be used to estimate the valid Reynolds number range from given values of the Schmidt number and the ratio between channel length and hydraulic diameter. While the diffusion-free RTD theory is not valid for gas flows, it is a reasonable approximation for liquid flows where the Schmidt number is large.
4. The present theory is not restricted to Newtonian fluids. Instead the results may readily be utilized to compute the RTD of any fully

developed laminar flow in a rectangular channel, whose velocity profile can be described or adequately fitted by Eq. (12).

5. The method presented in Section 2.2 for determining the cumulative RTD from a given cross-sectional velocity profile may be applied for laminar flow in straight channels with other cross-sectional shape as well. While it may seldom be possible to solve the resulting integrals analytically, this can be done numerically. The family of RTD curves proposed in Eq. (35) may then be used to fit the numerical data.

Notation

A	area of channel cross section, m^2
a	parameter in Gauss hypergeometric function, $a \equiv 1/m$, dimensionless
b	parameter in Gauss hypergeometric function, $b \equiv 1/n$, dimensionless
c	parameter in Gauss hypergeometric function, $c \equiv 1+a+b$, dimensionless
d	diameter of circular pipe, m
d_h	hydraulic diameter of rectangular channel, $d_h \equiv 4hw/(h+w)$, m
D	diffusion coefficient, m^2/s
E	differential RTD function, 1/s
E_θ	non-dimensional differential RTD function, $E_\theta \equiv t_m E$, dimensionless
\tilde{E}_θ	model RTD function, dimensionless
F	cumulative RTD function, dimensionless
${}_2F_1$	Gauss hypergeometric function
h	channel half-height, m
L	channel length, m
L_e	entrance length, m
m	exponent in the Purday velocity profile, dimensionless
n	exponent in the Purday velocity profile, dimensionless
Pe_h	Peclet number, $Pe_h \equiv d_h U_m / D$, dimensionless
Q	volumetric flow rate, m^3/s
Re_h	Reynolds number, $Re_h \equiv d_h U_m / \nu$, dimensionless
Sc	Schmidt number, $Sc \equiv \nu / D$, dimensionless
t	time or residence time, s

t_F	first appearance time, s
t_m	mean residence time, s
u	axial velocity, m/s
U_{\max}	maximum axial velocity, m/s
U_m	mean axial velocity, m/s
V	reactor volume, m ³
w	channel half-width, m
y	co-ordinate in channel cross-section, m
Y	Non-dimensional co-ordinate in channel cross-section, $Y \equiv y / h$, dimensionless
z	co-ordinate in channel cross-section, m
Z	Non-dimensional co-ordinate in channel cross-section, $Z \equiv z / w$, dimensionless

Greek letters

α, β, γ	general parameters in Gauss hypergeometric function, dimensionless
Γ	Gamma function
θ	non-dimensional residence time, $\theta \equiv t / t_m$, dimensionless
θ_F	non-dimensional first appearance time, dimensionless
Θ	$\Theta \equiv 1 - \theta_F / \theta$, dimensionless
λ	velocity ratio, $\lambda \equiv u / U_{\max} = \theta_F / \theta$, dimensionless
ν	kinematic viscosity, m ² /s
σ_θ^2	variance of differential RTD, dimensionless
χ	aspect ratio, $\chi \equiv h / w$, dimensionless

Subscripts and superscripts

F	first appearance
max	maximum value
m	mean value
λ	constant value of λ
○	circular channel
□	square channel
▭	rectangular channel
	planar channel

Abbreviations

RTD	residence time distribution
PNL	Purday-Natarajan-Lakshmanan

Appendix: Properties of the Gauss hypergeometric function

In this Appendix we list some properties of the Gauss hypergeometric function ${}_2F_1$.

For further information we refer to textbooks, e.g. Andrews (1998) and Andrews et al. (1999). Special values of the Gauss hypergeometric function are

$${}_2F_1(\alpha, \beta; \gamma; 0) = 1 \quad (\text{A.1})$$

and by the Gauss hypergeometric theorem

$${}_2F_1(\alpha, \beta; \gamma; 1) = \frac{\Gamma(\gamma)\Gamma(\gamma - \alpha - \beta)}{\Gamma(\gamma - \alpha)\Gamma(\gamma - \beta)} \quad (\text{A.2})$$

The rule for differentiation of the Gauss hypergeometric function is

$$\begin{aligned} \frac{d}{dx} {}_2F_1(\alpha, \beta; \gamma; x) &= \frac{\alpha\beta}{\gamma} {}_2F_1(\alpha + 1, \beta + 1; \gamma + 1; x) \\ &= \frac{\alpha}{x} [{}_2F_1(\alpha + 1, \beta; \gamma; x) - {}_2F_1(\alpha, \beta; \gamma; x)] \\ &= \frac{\beta}{x} [{}_2F_1(\alpha, \beta + 1; \gamma; x) - {}_2F_1(\alpha, \beta; \gamma; x)] \end{aligned} \quad (\text{A.3})$$

For the latter two identities see Eq. (9.14) and (9.15) in the book of Andrews (1998).

From Oberhettinger (1972) it is by Eq. (15.2.23)

$${}_2F_1(\alpha, \beta + 1; \gamma; x) = \frac{\beta - (\gamma - \alpha)x}{\beta(1-x)} {}_2F_1(\alpha, \beta, \gamma; x) + \frac{(\gamma - \alpha)(\gamma - b)}{\beta\gamma} \frac{x}{1-x} {}_2F_1(\alpha, \beta; \gamma + 1; x) \quad (\text{A.4})$$

and by Eq. (15.2.25)

$${}_2F_1(\alpha, \beta + 1; \gamma + 1; x) = -\frac{\gamma}{\gamma - \alpha} \frac{1-x}{x} {}_2F_1(\alpha, \beta + 1, \gamma; x) + \frac{\gamma}{\gamma - \alpha} \frac{1}{x} {}_2F_1(\alpha, \beta; \gamma; x) \quad (\text{A.5})$$

Introducing Eq. (A.4) in Eq. (A.5) gives

$${}_2F_1(\alpha, \beta + 1; \gamma + 1; x) = \frac{\gamma}{\beta} {}_2F_1(\alpha, \beta, \gamma; x) - \frac{\gamma - \beta}{\beta} {}_2F_1(\alpha, \beta; \gamma + 1; x) \quad (\text{A.6})$$

References

Adeosun, J.T., Lawal, A., 2009. Numerical and experimental studies of mixing characteristics in a T-junction microchannel using residence-time distribution. *Chem. Eng. Sci.* 64, 2422–2432.

Andrews, L.C., 1998. *Special functions of mathematics for engineers*, second ed. Oxford University Press, Oxford.

Andrews, G.E., Askey, R., Roy, R., 1999. *Special functions*, Cambridge University Press, Cambridge.

Aubin J., Prat, L., Xuereb, C., Gourdon, C., 2009. Effect of microchannel aspect ratio on residence time distributions and the axial dispersion coefficient. *Chem. Eng. Process.* 48, 554–559.

Bird, R.B., Stewart, W.E., Lightfoot, E.N., 2002. *Transport phenomena*, second ed. Wiley, New York, pp. 516–517.

Bošković, D., Loebbecke, S., 2008. Modelling of the residence time distribution in micromixers. *Chem. Eng. J.* 135S, S138–S146.

Bosworth, R.C.L., 1948. Distribution of reaction times for laminar flow in cylindrical reactors. *Phil. Mag.* 40, 847–862.

Cantu-Perez, A., Barrass, S., Gavriilidis, A., 2009. Residence time in microchannels: comparison between channels with herringbone structures and a rectangular channel. *Chem. Eng. J.*, doi:10.1016/j.cej.2009.07.023.

McComas, S.T., 1967. Hydrodynamic entrance lengths for ducts of arbitrary cross section. *ASME J. Basic Eng.* 89, 847–850.

Dankwerts, P.V., 1953. Continuous flow systems – Distribution of residence times. *Chem. Eng. Sci.* 2, 1–13.

Desmet, G., Baron, G.V., 2002. Chromatographic explanation for the side-wall induced band broadening in pressure-driven and shear-driven flows through channels with a high aspect-ratio rectangular cross-section. *J. Chromatogr. A* 946, 51–58.

Doshi, M.R., Daiya, P.M., Gill, W.N., 1978. Three-dimensional laminar dispersion in open and closed rectangular conduits. *Chem. Eng. Sci.* 33, 795–804.

Fogler, H.S., 1992. *Elements of chemical reaction engineering*, second ed. PTR Prentice Hall, Englewood Cliffs.

Forrey, R.C., 1997. Computing the hypergeometric function. *J. Comp. Phys.* 137, 79–100. (Source code available online at <http://physics.bk.psu.edu/codes/codes.html>).

Ham J.-H., Platzer, B., 2004. Semi-empirical equations for residence time distributions in disperse systems – Part 1: Continuous phase. *Chem. Eng. Technol.* 27, 1172–1178.

Hetsroni, G., Moysak, A., Pogrebnyak, E., Yarin, L.P., 2005. Fluid flow in micro-channels. *Int. J. Heat Mass Transf.* 48, 1982–1998.

Holmes D.B., Vermeulen, J.R., 1968. Velocity profiles in ducts with rectangular cross sections. *Chem. Eng. Sci.* 23, 717–722.

Levenspiel, O., 1979. *The chemical reactor omnibook*, OSU Book Stores Inc., Corvallis, p. 68–11.

Levenspiel, O., 1999. *Chemical reaction engineering*, third ed. Wiley, New York.

Lohse, S., Kohnen, B.T., Janasek, D., Dittrich, P.S., Franzke, J., Agar, D.W., 2008. A novel method for determining residence time distribution in intricately structured microreactors. *Lab Chip* 8, 431–438.

Morini, G.L., 2004. Laminar liquid flow through silicon microchannels. *J. Fluids Eng.* 126, 485–489.

Natarajan, N.M., Lakshmanan, S.M., 1972. Laminar flow in rectangular ducts: prediction of velocity profiles & friction factor. *Ind. J. Technol.* 10, 435–438.

Nauman, E.B., 1977. The residence time distribution for laminar flow in helically coiled tubes. *Chem. Eng. Sci.* 32, 287–293.

Nauman, E.B., 2008. Residence time theory. *Ind. Eng. Chem. Res.* 47, 3752–3766.

Nigam, K.P.D., Saxena, A.K., 1986. Residence time distribution in straight and curved tubes, in: ed. Chermisinoff, N.P. (Ed.), *Encyclopedia of Fluid Mechanics* 1, Gulf Publishing Co., Houston, pp. 675–762.

Oberhettinger, F. 1972. Hypergeometric functions, in: Abramowitz, M. and Stegun, I.A. (Eds.), *Handbook of mathematical functions with formulas, graphs, and mathematical tables*, tenth printing, National Bureau of Standards Applied Mathematical Series 55, GPO Bookstore, p. 558.

Probstein, R.F., 2003. *Physicochemical hydrodynamics*, second ed. Wiley, p. 86.

Purday, H.F.P., 1949. *An introduction to the mechanics of viscous flow*, Dover Publications, New York, p. 16.

Saxena, A.K., Nigam, K.P.D., 1983. Laminar dispersion in helically coiled tubes of square cross section. *Can. J. Chem. Eng.* 61, 53–57.

Shah, R.K., London, L., 1978. Laminar flow forced convection in ducts, Academic Press, New York, p. 198.

Shaw, D.A., Hanratty, T.J., 1977. Turbulent mass transfer rates to a wall for large Schmidt numbers. *AIChE J.* 23, 28–37.

Spiga, M., Morini, G.L., 1994. A symmetric solution for velocity profile in laminar flow through rectangular ducts. *Int. Commun. Heat Mass Transf.* 21, 469–375.

Stief, T., Schygulla, U., Geider, H., Langer, O.-U., Anurjew, E., Brandner, J., 2008. Development of a fast sensor for the measurement of the residence time distribution of gas flow through microstructured reactors. *Chem. Eng. J.* 135S, S191–S198.

Trachsel, F., Günther, A., Khan, S., Jensen, K.F., 2005. Measurement of residence time distribution in microfluidics systems. *Chem. Eng. Sci.* 60, 5729–5737.

Trivedi, R.N., Vasudeva, K., 1974. RTD for diffusion free laminar flow in helical coils. *Chem. Eng. Sci.* 29, 2291–2295.

Vikhansky, A., 2009. Taylor dispersion in shallow micro-channels: aspect ratio effect. *Microfluid Nanofluid* 7, 91–95.

Wibel, W., Ehrhard, P., 2009. Experiments on the laminar/turbulent transition of liquid flows in rectangular microchannels. *Heat Transf. Eng.* 30, 70–77.

Wörner, M., Ghidersa, B, Onea, A., 2007. A model for the residence time distribution of bubble train flow in a square mini-channel based on direct numerical simulation results. *Int. J. Heat Fluid Flow* 28, 83–94.

Figure captions

Fig. 1: Sketch of rectangular channel with dimensions and co-ordinate system.

Fig. 2: Dependence of the non-dimensional first appearance time $\theta_{F_{\square}}$ on the aspect ratio χ . Comparison of the approximations by Purday (1949) and Natarajan and Lakshmanan (1972) with exact values (Shah and London, 1978) and the fitting curve of Spiga and Morini (1994).

Fig. 3: RTD curves for laminar flow in circular and rectangular channels with different aspect ratio: cumulative RTD (a) and differential RTD in linear (main figure) and log-log scale (inset figure) (b).

Fig. 4: Non-dimensional differential RTD for a square channel. Comparison of the PNL-RTD (Eq. (31)) with the correlation of Saxena and Nigam (1983) (derivative of Eq. (11)) and with the present simplified model (Eq. (37)) for three different values of p .

Fig. 5: Range of validity (enclosed area) of pure convective RTD theory for $Sc = 1000$ and rectangular channels with different aspect ratio (s.l.d. = significant longitudinal diffusion).

Figures

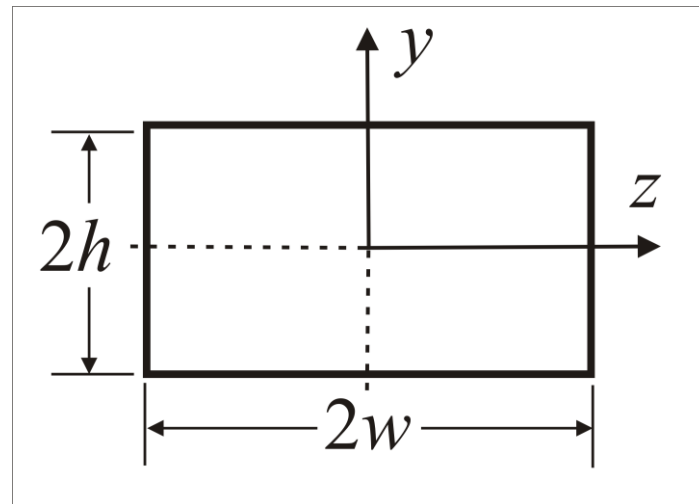


Fig. 1: Sketch of rectangular channel with dimensions and co-ordinate system.

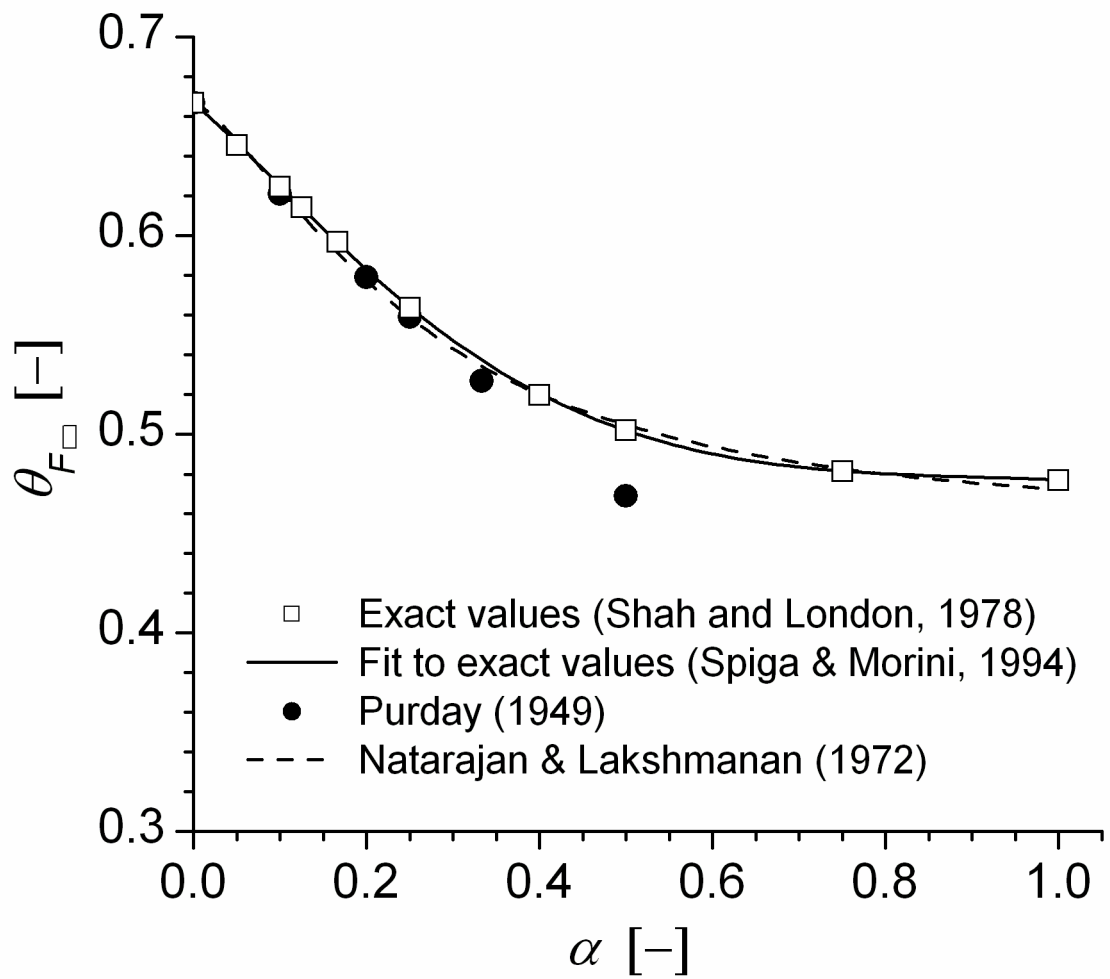


Fig. 2: Dependence of the non-dimensional first appearance time $\theta_{F_{\square}}$ on the aspect ratio χ . Comparison of the approximations by Purday (1949) and Natarajan and Lakshmanan (1972) with exact values (Shah and London, 1978) and the fitting curve of Spiga and Morini (1994).

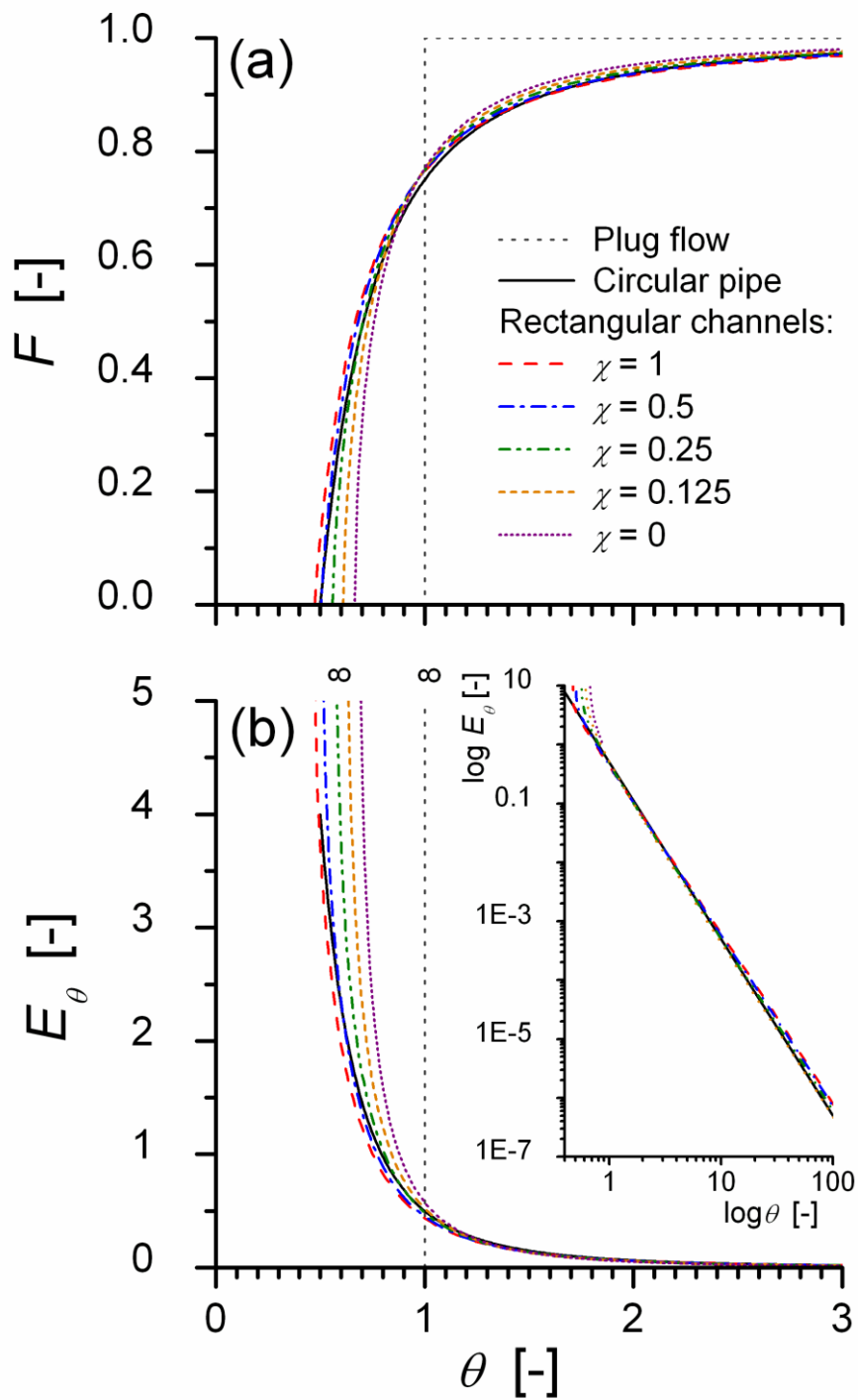


Fig. 3: RTD curves for laminar flow in circular and rectangular channels with different aspect ratio: cumulative RTD (a) and differential RTD in linear (main figure) and log-log scale (inset figure) (b).

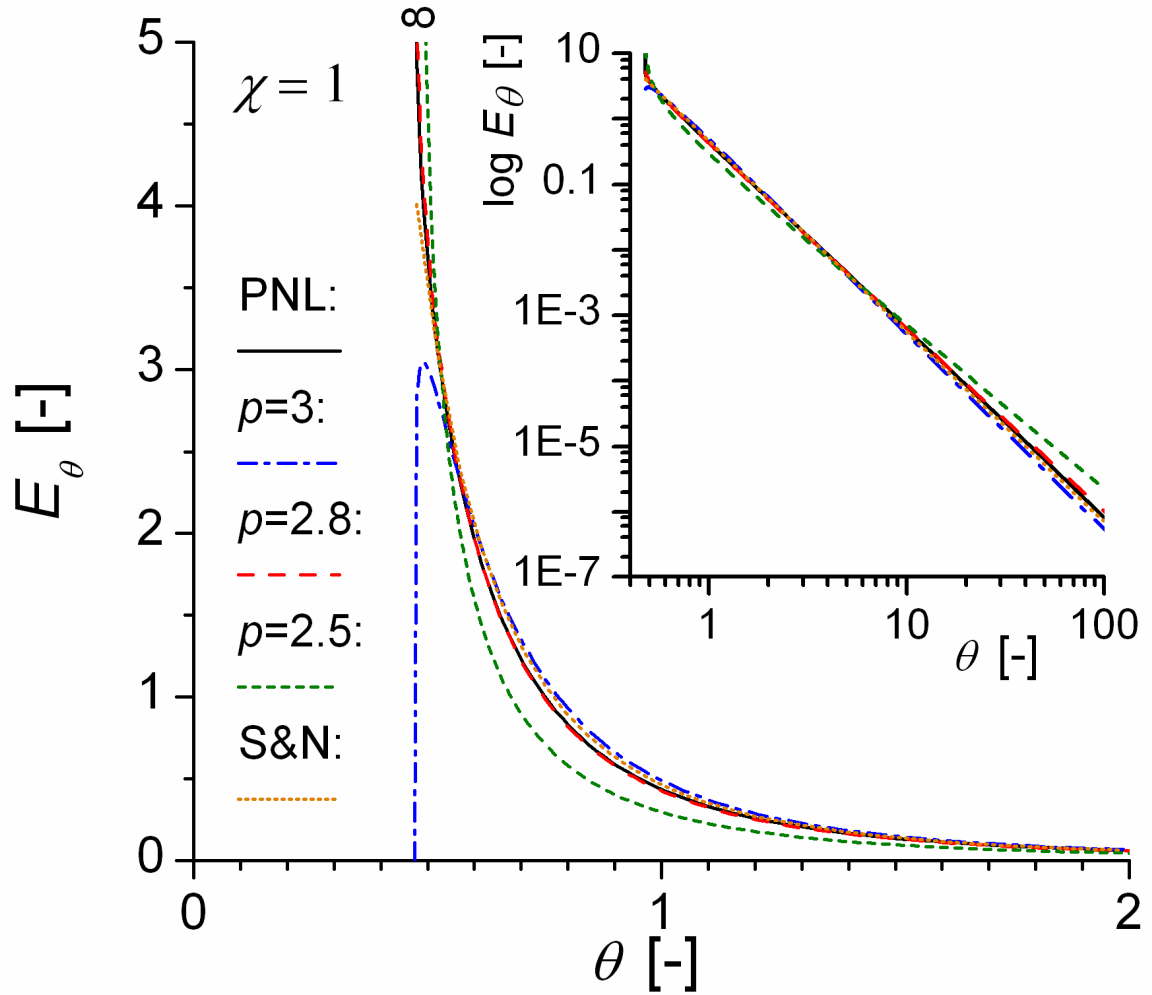


Fig. 4: Non-dimensional differential RTD for a square channel. Comparison of the PNL-RTD (Eq. (31)) with the correlation of Saxena and Nigam (1983) (derivative of Eq. (11)) and with the present simplified model (Eq. (37)) for three different values of p .

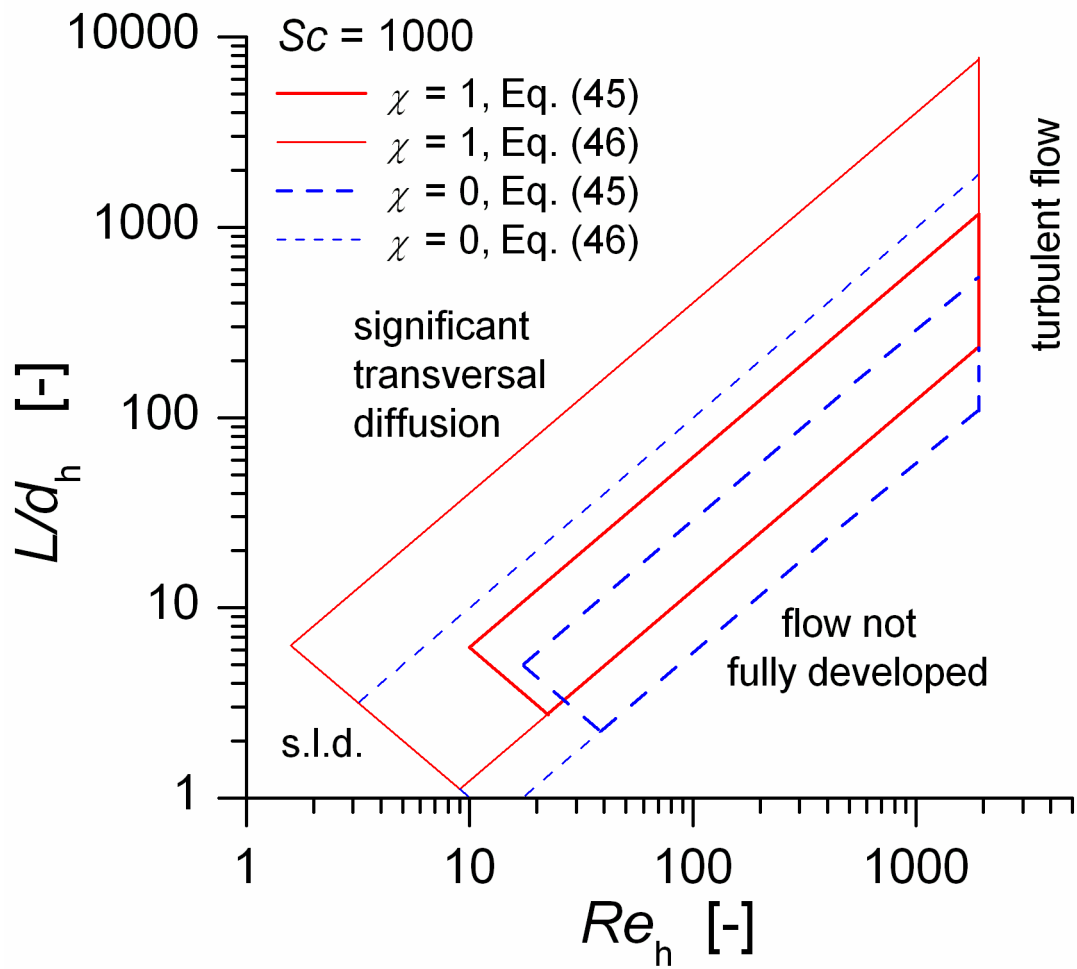


Fig. 5: Range of validity (enclosed area) of pure convective RTD theory for $Sc = 1000$ and rectangular channels with different aspect ratio (s.l.d. = significant longitudinal diffusion).

Tables

Tab. 1: Exponents m and n from Purday (1949) and Eq. (38) by Natarajan and Lakshmanan (1972) and comparison of the respective values of $\theta_{F\Box}$ with exact data from Shah and London (1978) for different values of the aspect ratio χ .

Variable	Reference	$1/\chi$						
		1	2	3	4	5	10	∞
m	Purday	–	2.37	3.78	5.19	6.60	13.60	∞
	N&L	2.2	3.02	4.03	5.18	6.46	14.26	∞
n	Purday	2	2	2	2	2	2	2
	N&L	2.2	2.05	2	2	2	2	2
θ_F	Purday	–	0.469	0.527	0.559	0.579	0.621	0.667
	N&L	0.473	0.505	0.534	0.559	0.577	0.623	0.667
	Exact (S&L)	0.477	0.502	–	0.564	–	0.625	0.667